Reduction of Norwegian and Indian ilmenite with carbon monoxide and hydrogen gas blends

STEPHEN LOBO*[1], LEIV KOLBEINSEN[1] and STIAN SEIM[2]

[1] *Norwegian University of Science and Technology, 7491, Trondheim, Norway*

[2] *TiZir Titanium and Iron, 5770, Tyssedal, Norway*

*corresponding author, stephen.lobo@ttinorway.com, Naustbakken 1, 5770 Tyssedal, Norway, tlf. +47 9009 1185

Stephen Lobo completed his PhD at the Norwegian University of Science and technology in November 2015. He has worked for four years studying and modelling the reduction of ilmenite using carbon monoxide and hydrogen blends. He is currently a metallurgist at TiZir Titanium & Iron in Tyssedal, Norway.

Reduction of Norwegian and Indian ilmenite with carbon monoxide and hydrogen gas blends

Synthesis gas, produced from natural gas, can be used to minimize coal consumption and carbon dioxide emissions during the processing of ilmenite. Two different ilmenite ores have been reduced with carbon monoxide and hydrogen mixtures to investigate the effects of temperature and gas composition on the final product. Thermogravimetric analysis was used to observe the reaction progress. Experimental work revealed that between 900 and 1000 °C the hydrogen content in the gas has an equally significant effect as the temperature. Statistical analysis determined that the source of the ore did not have a significant effect on the reaction rate. Armalcolite is one of the main products of pre-reduction in addition to metallic iron and rutile from these ilmenite concentrates. There is also some indication that titanium dioxide is reduced. Optical microscope images revealed that increasing amounts of hydrogen resulted in smaller more uniformly distributed metallic iron particles.

Keywords: ilmenite; pre-reduction; gas-solid reactions; syngas; natural gas;

Introduction

Ilmenite, $FeTiO_3$, is a major mineral source of titanium dioxide, TiO_2. Iron oxides in ilmenite can be metallised by selective reduction, commonly known as pre-reduction, leaving behind TiO_2 and metallic iron. These can be separated by melting. Reduction of iron in ilmenite is carried out using carbon monoxide gas created from partial combustion of coal. To decrease CO_2 emissions, natural gas can substitute coal as a reducing agent. Natural gas, primarily CH_4, can be reformed to so-called synthesis gas, a mixture of carbon monoxide, CO, and hydrogen, H_2.

Previous works have studied reduction of ilmenite using either carbon monoxide or hydrogen gas but few works have studied a mixture of the two. Investigations of reduction with H_2 have concluded that reactions occur faster than with CO.[1, 2] There is also potential for performing reduction at lower temperatures using H_2, however,

lowering the temperature will also slow the reaction due to kinetic factors. It has been seen in most cases that solid-state ilmenite reduction is controlled by both chemical reactions and mass transport, that is, mixed-controlled.[3] It has been reported that reduction with CO tends to result in coarse iron precipitates around the edges of product particles.[4] This stands in contrast to reduction with H_2 which gives finely distributed iron particles throughout the product.[1, 5]

The use of natural gas for reduction is well established in the iron ore industry for the production of direct-reduced iron, DRI. Pre-reduction of ilmenite can be compared to this process since it is mainly iron oxides which are reduced. A major difference, however, is that a stronger reducing atmosphere is necessary to carry-out ilmenite pre-reduction due to the presence of titanium and the high stability of iron-titanium intermediate oxides. These iron-titanium oxides are specified in Figure 1 as pseudobrookite (Fe_2TiO_5 and $FeTi_2O_5$), ilmenite ($FeTiO_3$) and ulvöspinel (Fe_2TiO_4).

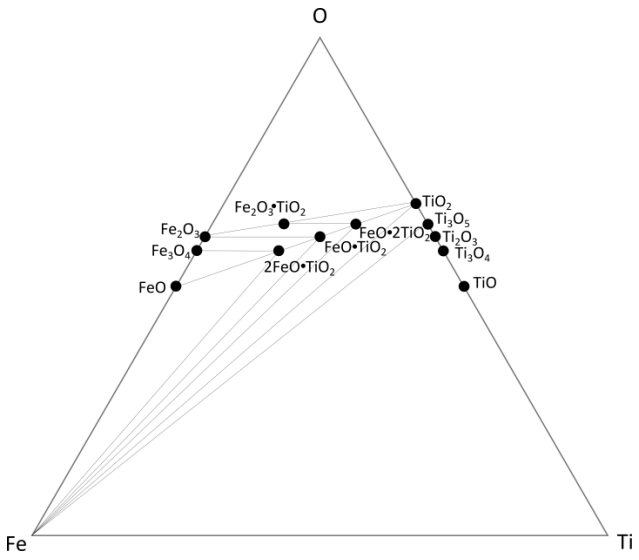

Figure 1. Relevant compounds for the reduction of ilmenite

In addition, solid solutions are often favourable along lines which contain equal ratios of metallic cations (M) and oxygen (O), i.e. M_3O_5, M_2O_3 and M_3O_4.

Previous work reports that oxidising ilmenite prior to reduction (preoxidation) increases the final conversion degree and/or rate.[6, 7] Therefore, the starting point for reduction is expected to be a point along the Fe_2O_3-TiO_2 line dependent on Fe and Ti content as well as the degree of oxidation.

Reactions (1) and (2) are reported to occur during reduction of preoxidised ilmenite with a reducing gas R (either CO or H_2) .[6-9]

$$Fe_2TiO_5 + TiO_2 + R \rightarrow 2FeTiO_3 + RO \quad (1)$$

$$FeTiO_3 + R \rightarrow Fe + TiO_2 + RO \quad (2)$$

Some studies have also suggested tetravalent titanium can be reduced to trivalent titanium.[5, 10] This probably occurs after iron is completely metallised.[5] However, trivalent titanium is not present as a distinct phase. Instead, it is a part of another oxide solution, for example the M_3O_5 or M_2O_3 system.[10] Another possibility is the formation of so-called Magneli phases which are lower titanium oxides with the general formulaTi_nO_{2n-1}.

Impurities have also been found to affect the reduction behaviour of ilmenite. There is evidence that magnesium, Mg, increases the stability of the M_3O_5 phase.[10, 11] This means that some of the iron remains in the oxide phase and armalcolite ($(Mg,Fe)Ti_2O_5$) ends up as a second oxide product. The presence of impurities has also been reported to lower the activity of iron in the oxide phase thereby lowering the reaction potential, slowing the reaction rate and decreasing the final conversion degree.[7] Studies have concluded that the morphology of iron formed during reduction with H_2 is different than that when CO is involved.[1, 12] H_2 reduction favours many smaller iron particles sometimes within the grain itself, whereas CO reduction produces larger iron particles located near the grain boundaries.[1, 8]

As mentioned previously, the presence of H_2 gas and higher temperatures increases the reaction rates, but the degree of influence from each variable has not been investigated. By factorial design, the effect of temperature and gas composition have been studied in this work. The factorial design makes use of statistics to create an empirical model based on strategically manipulated variables.[13] In short, the method uses high and low values for each of the variables and experiments are performed at all combinations of these conditions. Using this method, the effects of the variables can be investigated over a wide range. A quantitative value, a response variable, is obtained from each experiment, measured and then used for statistical analysis.

Experimental methods

Ilmenite pellets were made and preoxidised by Minpro AB. The ilmenite was sourced from two mines, a Norwegian rock deposit and an Indian sand deposit. The pellets were oxidised at a maximum temperature of 950 °C. The chemical analysis of the oxidised material was conducted by X-ray fluorescence. A Philips PW204 XRF at the TiZir Titanium and Iron labs was used for analysis. It can be seen from the analysis in Table 1 that one main difference is that the Norwegian ore contains considerably more MgO than the Indian. The iron content between the two ores is very similar. The amounts of di- and trivalent iron were determined using titration, also known as wet chemical analysis.

Table 1 Chemical analysis of oxidised ilmenite (wt.-%)

	%TiO_2	%Fe(total)	%FeO	%Fe_2O_3	%MnO	%CaO	%MgO	%SiO_2	%Al_2O_3	%Cr_2O_3	%V_2O_5	%Nb	%P_2O_5
Norwegian	42.8	35.5	5.5	44.6	0.3	0.26	3.6	2.6	0.7	0.13	0.2	0.01	0.015
Indian	49.5	34.4	5.1	43.5	0.6	0.06	0.7	0.8	0.6	0.08	0.2	0.09	0.023

X-ray diffraction prior to reduction indicated that both oxidised ores consisted of ilmenite, hematite, armalcolite, pseudorutile and rutile. The Norwegian ore also had trace amounts of enstatite ($Mg_{0.56}Fe_{0.44}SiO_3$).

The porosity and density of the oxidised pellets was also measured and are reported in Table 2. An AccuPyc II 1340 pycnometer with helium gas was used to measure the absolute density and a GeoPyc 1360 envelope density analyser was used to measure the apparent density. The two values are then used to calculate the porosity.

Table 2 Porosity of oxidised ilmenite

Ore	Absolute Density (g cm^{-3})	Apparent Density (g cm^{-3})	Porosity (%)
Norwegian	4.36	3.24	26.1
Indian	4.44	3.31	25.9

Table 3 Experimental conditions

Experiment number	Ore	Hydrogen content* (vol.-%)	Temperature (°C)
1	Indian	75%	1000
2	Indian	75%	900
3	Indian	25%	1000
4	Indian	25%	900
5	Norwegian	75%	1000
6	Norwegian	75%	900
7	Norwegian	25%	1000
8	Norwegian	25%	900
Test	Indian	50%	1000

*balance is CO

As reported in Table 3, the high and low values for H_2 content in the gas were 75 and 25 vol.-% with the balance consisting of CO and the temperature was either 1000 or 900 °C. All combinations of these high and low values were tested in four experiments. This was repeated for each ore giving a total of eight experiments. These experiments were analysed to create an empirical model. A ninth experiment was conducted, called Test, to test the validity of this model. In all cases, reduction lasted 2 hours and warming and cooling were carried out in an argon atmosphere. The total gas

flow for the experiments was 5 L min^{-1}. This is believed to be sufficient to ensure an unchanging composition of gas in the bulk flow and a constant boundary layer around the pellets.

Reduction was done in a thermogravimetric furnace (TGA) on 10-14 mm sized pellets in batches of approximately 200 g. A schematic of the crucible is given in Figure 2. Gas entered through the inlet and descended through the double wall, this served to preheat the gas. At the bottom, the gas ascended through the pellet bed which was sitting on a perforated stage. The crucible is constructed with 1mm 253MA high temperature stainless steel with a maximum operating temperature of more than 1100°C.

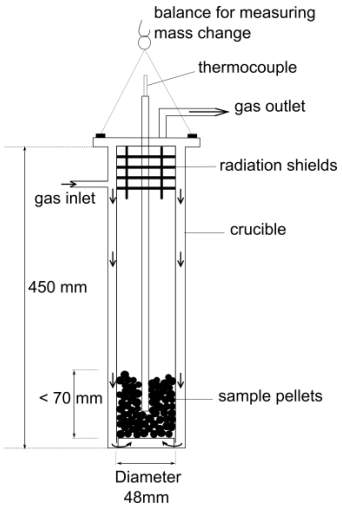

Figure 2. Schematic of TGA furnace used for reduction

Bronkhorst model F201c mass flow controllers were used to measure the gas before mixing. The gas mixture entered the crucible and was preheated through the double wall of the crucible. Then the gas flowed through a packed bed of pellets and exited the top of the crucible. The crucible was externally heated by an Entech VTF 80/15 furnace with a Kanthal element. Temperature was set by the furnace, however, it was measured by a thermocouple in the packed bed to observe the conditions in the pellet bed. Mass

change data during the experiments were measured by a PR2003DR Mettler Toledo mass balance and logged as a function of time. The conversion degree, d, was calculated according to Equation (3) where Δm is the mass change during the experiment and m_o is the total amount of oxygen in FeO and Fe_2O_3 at the start of the experiment. m_o is calculated based on the iron content from Table 1. Carbon deposition from CO gas is considered negligible based on previous work using the same apparatus and similar conditions.[2]

$$d = \left(\frac{\Delta m}{m_o} \right) 100 \qquad (3)$$

Minitab® 17 Statistical Software was used to analyse the response variables[14]. Regression analysis was performed according to the standard method of creating an empirical model and eliminating effects that produced high residuals.

X-ray diffraction was conducted on a Bruker D8 Advance with a Davinci design. The scans were completed from 5°-75° using a step size of 0.019° and 95.5 seconds per step. The resulting patterns were matched using Bruker Diffrac EVA software and the PDF® database[15].

Selected pellets were mounted in epoxy and polished. Optical micrographs were taken with a Olympus Bx51 light microscope equipped with a Jenoptik Progres Speed XTcore 5 camera and ProgRes CapturePro software.

Results

X-ray diffraction (XRD)

The X-ray diffraction analysis findings are listed in Table 4.

Table 4 Summary of X-ray diffraction analysis

Experiment Number		Type of phase				
		M_2O_3	**M_3O_5**	**Rutile**	**Iron**	**Trace Impurities**
1	(Indian)	…	$Mg_{0.31}Ti_{2.36}Fe_{0.33}O_5$	TiO_2	Fe	$MgSiO_3$, $Cr_{0.12}Ti_{0.78}O_{1.74}$
2		$TiMn_{0.2}Fe_{0.8}O_3$	…	TiO_2	Fe	…
3		$FeTiO_3$	$Mg_{1.2}Ti_{1.8}O_5$	$Ti_{0.98}O_2$	$Mn_{0.05}Fe_{0.95}$	…
4		$Ti_{0.96}Fe_{1.03}O_3$	…	TiO_2	$(Fe_{97}Mn_3)_{0.02}$	…
5	(Norwegian)	…	$Mg_{0.31}Ti_{2.36}Fe_{0.33}O_5$	TiO_2	$(Fe_{97}Mn_3)_{0.02}$	$Mg_2V_2O_7$
6		$Fe_{1.04}Ti_{0.96}O_3$	…	TiO_2	Fe	$(Fe,Mg)SiO_3$
7		$Fe_{1.04}Ti_{0.96}O_3$	$Mg_{0.31}Ti_{2.36}Fe_{0.33}O_5$	TiO_2	$Mn_{0.05}Fe_{0.95}$	$Mg_{0.75}Fe_{0.25}SiO_3$, $VMn_{0.5}Fe_{1.5}O_4$
8		$FeTiO_3$	…	$Ti_{0.928}O_2$	$Mn_{0.05}Fe_{0.95}$	$(Mg_{1.561}Fe_{0.439})Si_2O_6$, $Ca(Mg,Fe,Al)(Si,Al)_2O_6$
Test (Indian)		$Ti_{0.96}Fe_{1.03}O_3$	$Mg_{0.5}Ti_2Fe_{0.5}O_5$	$Ti_{0.928}O_2$	Fe, $Ti_{0.025}Fe_{0.975}$	$Al_2(SiO_4)$

The analysis was done qualitatively therefore it was not possible to state the exact amounts of each phase, however, the trace impurity peaks, i.e. impurity peaks not in the Mg-Fe-Ti-O sytem, were very low and therefore they will not be included in further discussion. As an example, the diffraction pattern of the Test sample is shown in Figure 3. Here is it seen that the two visible $Al_2(SiO_4)$ peaks are low and one is not large enough to be distinguished from the background. It can also be seen that the M_3O_5 peaks are relatively low compared to the M_2O_3, rutile and iron peaks. This is due to the stability of the M_3O_5 phase which is explained later.

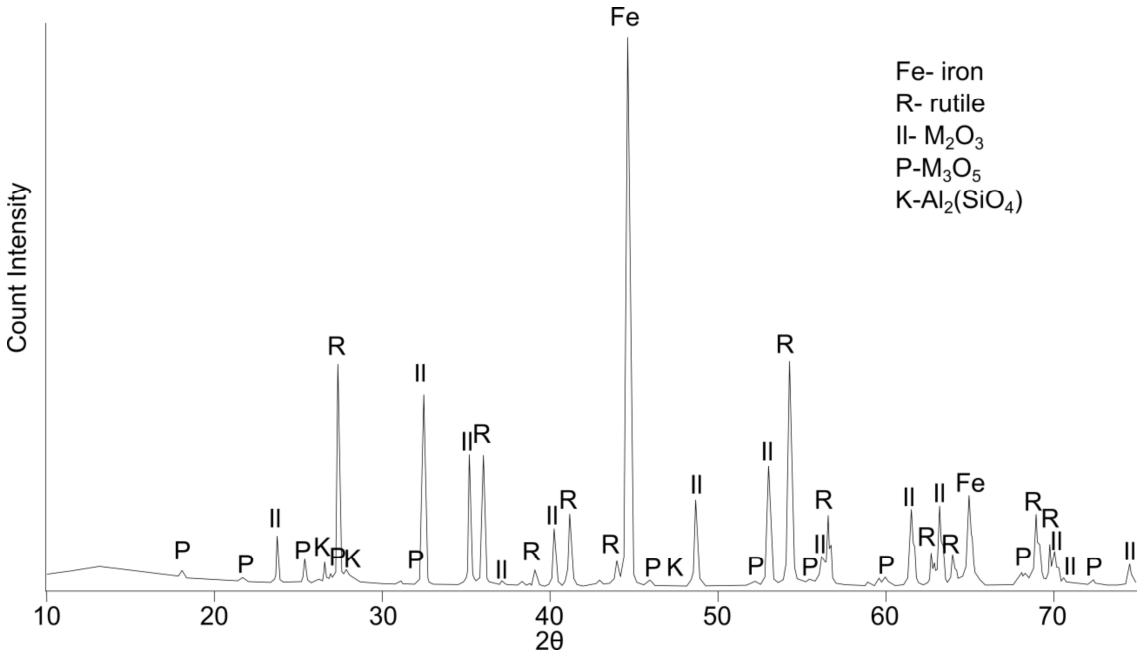

Figure 3. X-ray diffraction pattern from Test sample. Iron, Rutile and M_2O_3 peaks represent the major phases, some M_3O_5 phase is present as well as trace amounts of $Al_2(SiO_4)$ (kyanite).

In all experiments the end products included a metallic iron phase. All experiments also resulted in a rutile phase, however, the other oxide phases varied.

The high temperature, high H_2 content experiments did not contain any M_2O_3 phases, independent of ore type. The experiments at low temperature but high H_2 content (Experiments 2 and 6) contained no M_3O_5 whereas those at high temperature and low H_2 content (Experiments 3 and 7) contained both M_2O_3 and M_3O_5 phases. The low temperature, low H_2 content experiments (Experiments 4 and 8) resulted in M_2O_3 but no M_3O_5.

In Experiments 1, 5 and 7 the M_3O_5 phase probably contains a small amount of reduced Ti-oxides, if one assumes Mg and Fe are only present in their divalent state. This can be seen by re-writing the chemical formula $Mg_{0.31}Ti_{2.36}Fe_{0.33}O_5$ as

$(MgO)_{0.31}(FeO)_{0.33}(TiO_{1.847})_{2.36}$. The other possibility is that elemental Fe is present in the oxide phase or MgO has been reduced, however, this seems unlikely.

Thermogravimetric analysis

Conversion degree calculated according to Equation (3) as a function of time is plotted in Figure 4.

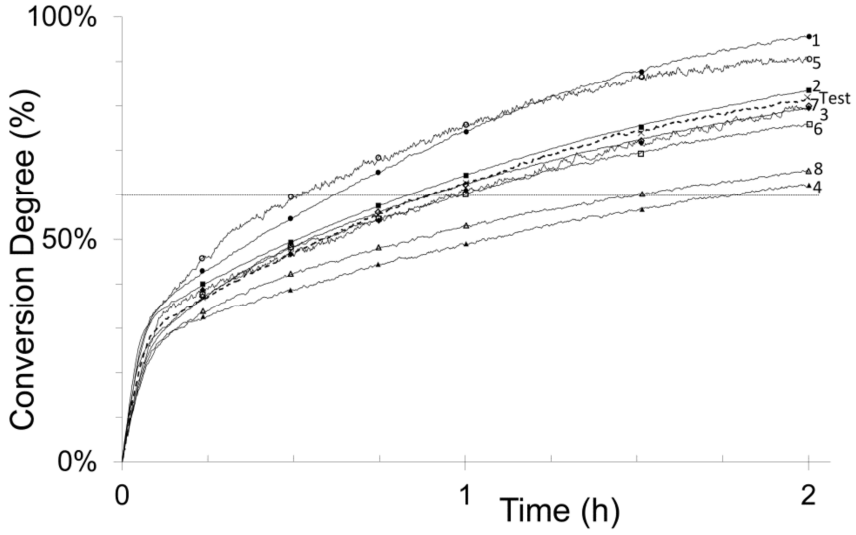

Figure 4. Conversion degree as a function of time for all experiments. The numbers correspond to the experiments listed in Table 3. Horizontal line corresponds to 60% reduction

As expected, high temperature and high H_2 content experiments reduced faster and achieved a greater final conversion degree. The high temperature, low H_2 content experiments (Experiments 3 and 7) appear to follow similar paths regardless of ore source. However, the low temperature, high H_2 content (2 and 6) are noticeably different for the different ores. The Test experiment falls near the middle of all curves. In all cases, two distinct regions of reduction are present. The initial reduction is very fast and the second stage is slower. Also, in all experiments, the first stage of reduction ends after approximately 4 minutes and 15 seconds.

Statistical analysis

Appropriate response variables for the statistical analysis were determined to be the final degree of conversion and amount of time taken to reach 60 %. These values are reported in Table 5.

Table 5 Response variables

Experiment number	Time taken to reach 60 % conversion (min.)	Final conversion degree (%)
1	36	62
2	49	80
3	56	83
4	105	96
5	30	65
6	58	80
7	53	76
8	87	90
Test	53	82

After entering these values into the software a model was made based on regression. The regression method took each of the individual variables into account, i.e. ore (O), H_2 content in the gas (G) and temperature (T) to derive an empirical model of the response variables. The interactions between the variables were also included, i.e. (O*G), (O*T), (G*T) and (O*G*T).

The variance between the model and the experimental results was used to eliminate terms which had little to no effect on the overall outcome. For the model in this work, all of the interaction terms and even the variable for ore were eliminated. The final model was only dependent on temperature and gas composition. All other terms were eliminated based on their p-values being lower than 0.05, a common threshold for statistical significance. Elimination of many variables led to a regression model containing coefficients with a high standard error. As seen in Tables 6 and 7, the

standard error for both models is very large. The coefficients from the standardised model were then transformed into real, non-standardised values to give an equation for the reduction model. The standardised model defines the low and high conditions as -1 and 1 respectively. This allows for the model to be analysed using an identical range for all the variables. In this case, the temperature range is 100°C and the hydrogen content is only 50 percentage points. Therefore, the standardised model gives an indication of their effects on with an identical range. It is easier to see the relative effects of the variables when using the standardised model. The non-standardised model, however, gives a real prediction for the given conditions.

Table 6 Standardised Coefficients for Regression (Final Conversion)

Term	Effect	Coefficient	Standard Error	p-value
Constant	…	0.790	0.0113	0.000
Hydrogen content	0.15	0.073	0.0113	0.001
Temperature	0.15	0.075	0.0113	0.001

Table 7 Standardised Coefficients for Regression (Time to reach 60% conversion)

Term	Effect	Coefficient	Standard Error	p-value
Constant	…	59.3	3.3	0.000
Hydrogen content	-32.0	-16.0	3.3	0.005
Temperature	-31.0	-15.5	3.3	0.006

The final conversion after 2 hours (R) in this regime as a function of H_2 gas content (H) in vol.-% and temperature (T) in Kelvin is given by Equation (4). This equation is presented using the non-standardised coefficients.

$$R = -1.189 + 0.0029H + 0.0015T \quad (4)$$

A similar analysis for the conversion times resulted in a similar regression model. The amount of time (t, min.) it takes for ilmenite to reach 60 % conversion under these

conditions can be approximated by Equation (5).

$$t = 470.4 – 0.640\ H - 0.31\ T \qquad (5)$$

According to Equations (4) and (5) the final conversion for the Test experiment the final conversion degree should be 87 % and 60 % conversion is reached after 44 minutes, compared to the 85 % and 48 minutes which were found experimentally.

Microscopic analysis

Analysis was also done with an optical microscope to investigate how iron formed in the pellet. Samples from Experiments 1 and 5 were selected as they underwent reduction at the highest temperature together with the highest H_2 content in the gas, the micrographs are displayed in Figures 5 and 6.

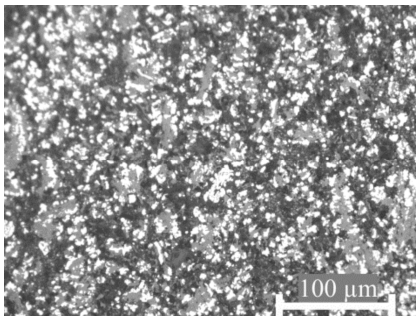

Figure 5. Optical micrograph near the outer layer of pellet from Experiment 1

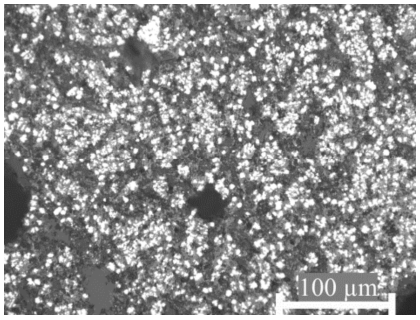

Figure 6. Optical micrograph near the outer layer of pellet from Experiment 5

Samples from Experiments 4 and 8 were also selected for analysis since they were the

exact opposite reducing conditions. These micrographs are reported in Figures 7 and 8.

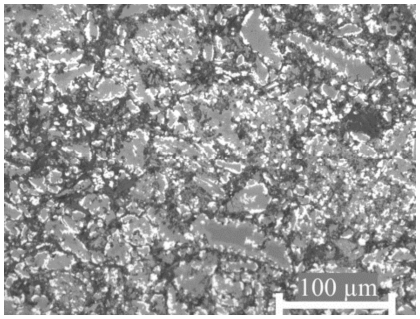

Figure 7. Optical micrograph near the outer edge of pellet from Experiment 4

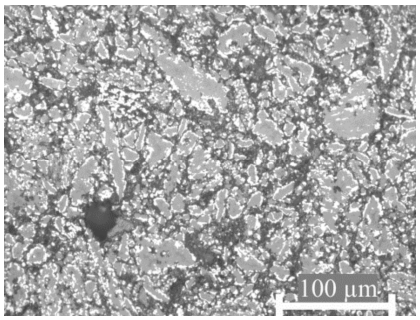

Figure 8. Optical micrograph near the outer edge of pellet from Experiment 8

Analysis was done near the outer edges of the pellets. The bright particles in the images are iron, the grey areas oxides phases and the black areas are pores. Light microscopy was not able to distinguish individual oxide phases.

Though the ilmenite ores come from different deposits, the morphology of the particles appears to be identical. There is no significant difference between the images from sand deposits and rock deposits.

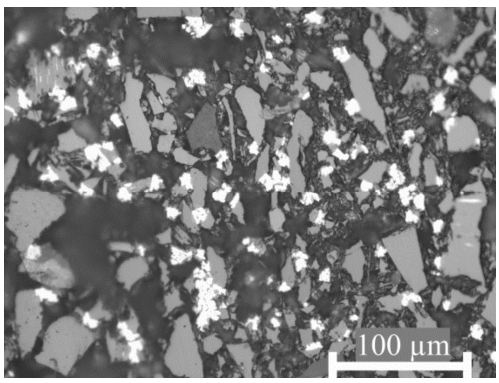

Figure 9. Optical micrograph near the centre of pellet from Experiment 1

The micrographs in Figures 5-8 reveal that at 1000 °C and 75 vol.-% H_2 in the gas, the iron forms in smaller particles. At 900 °C and 25 vol.-% H_2, the iron forms slightly larger granules and is mainly formed at particle boundaries.

By comparing Figure 5 and Figure 9, it is seen that the outer layer has smaller pores than the centre. This observation was made for several pellets. These effects are possibly due to the roasting (preoxidation) and pelletising steps. Despite the porosity differences, the centres of the pellets did not have as much metallic iron. Figure 9 indicates that very little iron formed in the centre and the iron that is formed is in large particles near the particle boundaries.

Discussion

The results confirm that an increase in H_2 and temperature increase the reaction rate and final conversion degree during ilmenite reduction. The errors in the regression models are quite large and therefore any quantitative analysis on the model would be dubious. There was a 2 % difference between the final conversion of the Test experiment and the model prediction. The difference for the time model was 8 % when compared to the Test experiment. However, the magnitudes of the coefficients are identical. This is evidence that the temperature and gas composition have equally important roles under these reduction conditions. Therefore, between 900 and 1000 °C, a reduction in temperature could be compensated for by an increase in H_2 content.

The ore type did not have a significant effect on the conversion rate. Although the Norwegian ore contained significantly more MgO and had a lower TiO_2 content, this was not enough to affect the model. Also, the X-ray diffraction results of the end products indicate that similar compounds are formed regardless of ore source if the temperature and gas composition during reduction are equal. Grey and colleagues have

reported that MgO can stabilise the M_3O_5 phase and this is verified in the results[10]. This is especially the case for high temperature and high H_2 content reduction where no ilmenite remains in the product. There was enough Mg to form M_3O_5, even though the Orissa ilmenite only contained 0.66% MgO. It is important to note that at low temperatures M_3O_5 was not formed regardless of gas composition. In these cases the Mg is suspected to be in the M_2O_3 phase.

The conversion degree of Experiments 2, 3, 6 and 7 were similar, however Experiments 2 and 6 did not result in any M_3O_5 phase. This result can be explained using the findings of Boroweic and Rosenqvist[11]. They report that the size of four phase region of M_2O_3-M_3O_5-Fe-TiO_2 depends very much on temperature. In the current work, the same four phase region is stable at 1000 °C but not at 900°C. Therefore at 900 °C only a three phase region of M_2O_3-Fe-TiO_2 is stable.

The shape of the conversion degree curves is in accordance with previous work[3, 16]. Initially, the reduction proceeds quickly due to low product layer resistance and high driving forces reducing Fe^{3+} to Fe^{2+}. The reduction then slows as mass transport through the product layer becomes more difficult and a higher reduction potential is needed to reduce Fe^{2+} to Fe.

The presence of $Mg_{0.31}Ti_{2.36}Fe_{0.33}O_5$ in the final product is an indication of titanium reduction. However, due to the very small amounts of reduced titanium species, analysis and identification is difficult. It is likely that some Ti^{4+} is reduced to Ti^{3+} however since it is not present as a pure phase it is difficult to detect.

Microscopic analysis confirms that iron formation on the particle boundaries is more favourable at higher CO concentrations and that H_2 enhances iron formation within the particles[12]. This is because the H_2/H_2O equilibrium creates a larger driving force for iron nucleation than the CO/CO_2 equilibrium at the same temperature. This

driving force is a function of the oxygen partial pressure in each of the respective equilibriums. As previous work concludes, iron formation during ilmenite reduction has three distinct parts: (1) induction of nucleation (2) acceleration due to mass transport and (3) deceleration due to consumption of reactants[4, 5]. The lower oxygen partial pressure created by the H_2/H_2O equilibrium increases the rate of induction, step (1), thereby creating more nucleation sites for iron. Then subsequent metallised iron does not have to diffuse as far during the acceleration step. For higher oxygen partial pressures such as those given by the CO/CO_2 equilibrium, nucleation occurs at particle boundaries due to the lower energy requirement. Since there are fewer nucleation sites, the size of the iron particles is larger when there is more CO and less H_2 in the reducing gas.

Analysis determined that a dense outer layer formed in the pellets during either pelletisation or preoxidation. Sintering of the outer layer of the pellet appears to hinder complete reactions at the centre of the pellet. Although the transport of gases in the porous centre should occur readily, the materials remain relatively unreacted. This is possibly due to product gases not being able to easily vacate the centre thereby stopping further reactions.

Porosity is one variable which was not manipulated in this work. The porosity between the two samples was initially quite similar. Previous studies report that ilmenite reduction is partially controlled by diffusion and therefore porosity is a significant variable and its effects should be studied further. The shape and size of pores is also important. Since gas-solid chemical reactions are assumed to take place on surfaces the specific surface area within a pellet is another important variable to consider. As seen in the micrographs, the porosity is inconsistent within the pellets adding further complexity to the mass transport mechanisms.

It has also been seen that due to the randomness of pelletisation, the properties of pellets can vary from batch to batch and this can change the reduction behaviour. Limiting the model to only a few variables could therefore have eliminated other key variables from consideration.

Conclusions

From this series of experiments it is concluded in a CO-H_2 blend containing between 75 % and 25 % of each gas, gas composition has an equally significant effect on the reaction rate as temperature. There was no significant difference in reduction behaviour between the ore from the sand deposit and the rock deposit. The presence of magnesium has a very significant impact on the final products, even in small amounts. Armalcolite, an M_3O_5 phase, ends up in the final product as long as Mg is present in the ore. Since armalcolite contains iron, complete metallisation does not occur. It is seen that the M_3O_5 phase is also temperature dependant. At 900°C it does not co-exist with M_2O_3, TiO_2 and metallic iron.

Although there are signs of titanium reduction, analysis was not conclusive. The presence of impurities complicates analysis for reduced titanium species.

Additionally, iron forms along particle boundaries when CO is used due to higher oxygen partial pressures compared to when H_2 is used.

This work shows that the rate of reduction for ilmenite using a blend of CO and H_2 gases is mainly dependent on the gas mixture and the temperature. The results of this work can be used to further determine optimal conditions for ilmenite reduction and further investigate the mechanisms involved when using a mixture of gases.

Acknowledgements

The authors would like to thank the GASFERROSIL project (grant number: 224950/E30) financed by the Research Council of Norway for supporting this project. Edith Thomassen and Irene Braagstad of SINTEF Materials and Chemistry are also owed gratitude for their assistance during experimental work.

References

1. G. Östberg, 'Solid State Reduction of Ilmenite', *Jernkont. Ann.*, 1960, **144**(1), 46-76.
2. S. Lobo, L. Kolbeinsen, and S. Seim: 'Reduction of Ilmenite with Synthesis Gas', Heavy Minerals Conf. 2013, Vishakapatnam, India, 2013.
3. K. Sun, R. Takahashi, and J.-i. Yagi, 'Kinetics of the Oxidation and Reduction of Synthetic Ilmenite', *ISIJ Int.*, 1993, **33**(5), 523-528.
4. Y. Zhao and F. Shadman, 'Kinetics and Mechanism of Ilmenite Reduction with Carbon Monoxide', *AlChe J.*, 1990, **36**(9), 1433-1438.
5. Y. Zhao and F. Shadman, 'Reduction of Ilmenite with Hydrogen', *Ind. Eng. Chem. Res.*, 1991, **30**(9), 2080-2087.
6. D. G. Jones, 'Kinetics of Gaseous Reduction of Ilmenite', *J. Appl. Chem. Biotechnol.*, 1975, **25**, 561-582.
7. R. Merk and C. A. Pickles, 'Reduction of Ilmenite by Carbon Monoxide', *Can. Metall. Q.*, 1988, **27**(3), 179-185.
8. D. G. Jones, 'Optical microscopy and electron-probe microanalysis study of ilmenite reduction', *Trans. Inst. Min. Metall., Section C*, 1974, **83**(808), 1-9.
9. S. Itoh and A. Kikuchi, 'Reduction Kinetics of Natural Ilmenite Ore with Carbon Monoxide', *Mat. Trans., JIM*, 2001, **42**(7), 1364-1372.
10. I. E. Grey, A. F. Reid, and D. G. Jones, 'Reaction sequences in the reduction of ilmenite: 4- interpretation in terms of the Fe-Ti-O and Fe-Mn-Ti-O phase diagrams', *Trans. Inst. Min. Metall. C*, 1974, **83**(June), 105-111.
11. K. Borowiec and T. Rosenqvist, 'Phase Relations and Oxygen Potentials in the Fe-Ti-Mg-O System', *Scand. J. Metall.*, 1985, **14**, 33-43.
12. M. L. de Vries, I. E. Grey, and J. D. Fitzgerald, 'Crystallographic Control in Ilmenite Reduction', *Metall. Mater. Trans. B*, 2007, **38B**(2), 267-277.
13. G. E. P. Box, W. G. Hunter, and J. S. Hunter: 'Factorial Designs at Two Levels', in 'Statistics for Experimenters: An Introduction to Design, Data Analysis, and

Model Building', (eds. V. Barnett*, et al.*), 306-351; 1978, John Wiley & Sons, Inc.

14. Minitab Inc., *Minitab® 17 Statistical Software*. 2010.
15. JCPDS – International Centre for Diffraction Data, PDF-2 XRD database. 2014.
16. G. Bardi, D. Gozzi, and S. Stranges, 'High temperature reduction kinetics of ilmenite by hydrogen', *Mater. Chem. Phys.*, 1987, **17**, 325-341.